Available online at www.sciencedirect.com
ScienceDirect
Lithos 95 (2007) 399–414
LITHOS
www.elsevier.com/locate/lithos

Origin of potassic (C-type) adakite magmas: Experimental and field constraints

L. Xiao [a], J.D. Clemens [b,*]

[a] Faculty of Earth Science, China University of Geosciences, 388 Lumo Rd, Hongshan District, Wuhan 430074, China
[b] School of Earth Sciences & Geography, CEESR, Kingston University, Penrhyn Rd, Kingston-upon-Thames, Surrey KT1 2EE, UK

Received 14 December 2005; accepted 4 September 2006
Available online 30 October 2006

Abstract

The postcollisional, Mesozoic, C-type or high-K adakitic intrusions (K-adakites) of China lack either temporal or spatial association with subduction and have K_2O/Na_2O around unity. Otherwise, their geochemistry is very similar to ordinary adakites. New experimental data, geological observations and theoretical considerations lead us to suggest that these K-adakites were high-*T* (>1050 and probably >1075 °C), rather hydrous magmas (~6 wt.% H_2O) produced by fluid-absent partial melting of metatonalites, meta-andesites, or possibly potassic metabasalts at pressures exceeding 2 GPa. Their peculiar chemistry is a consequence of both the elevated K_2O/Na_2O in the protolith and the very high pressure of partial melting. The most likely tectonic setting is one of extreme crustal thickening followed by delamination of the eclogitic keel and partial melting of this continental crustal material at mantle depths, with high mantle heat flow, during orogenic collapse.
© 2006 Elsevier B.V. All rights reserved.

Keywords: Adakite; K-rich; Granite; Petrogenesis

1. Introduction — the adakite problem and potassic (C-type) adakites

Adakites are volcanic and intrusive igneous rocks with $SiO_2 \geq 56$ wt%, $Al_2O_3 \geq 15$ wt%, K_2O/Na_2O typically < 0.6, high La/Yb and Sr/Y ratios coupled with strong depletion in Yb, Y and HFSE, and typically found in island and continental arc settings (see e.g., Defant and Drummond, 1990; Castillo, 2006). Their geochemical characteristics suggest an origin by partial melting of metabasaltic crust at pressures high enough to stabilise garnet. Adakites that occur along convergent plate boundaries have been interpreted as melts of the down-going slab (e.g., Drummond and Defant, 1990). The thermal models of Peacock et al. (1994) showed that slab melting should be restricted to unusually hot subduction zones. Various authors have suggested settings in which this could occur — subduction initiation, subduction collision, tearing of the slab and shallowing of the subduction angle (e.g., Sajona et al., 1993, 1994, 2000; Gutscher et al., 2000; Yogodzinski et al., 2001; Beate et al., 2001; Bourdon et al., 2002; Calmus et al., 2003). Bindeman et al. (2005) surveyed the O isotope systematics of a wide variety of subduction-related adakites and found little evidence of the supposed slab component. They comment (p. 481) that "…adakites might not be slab melts at all, and instead come from differentiation and/or partial melting processes near the base of the arc crust in the over-riding

* Corresponding author.
E-mail address: j.clemens@kingston.ac.uk (J.D. Clemens).

0024-4937/$ - see front matter © 2006 Elsevier B.V. All rights reserved.
doi:10.1016/j.lithos.2006.09.002

plate." Atherton and Petford (1993) suggested melting of young lower crustal rocks, in the upper plate, as an alternative to the slab melting hypothesis, and direct geological evidence for this alternative mechanism was presented first by Stevenson et al. (2005). Macpherson et al. (2006) presented evidence that some adakitic melts are produced by fractional crystallisation of garnet-bearing assemblages from basaltic arc magmas that were generated from fluid-modified mantle.

The issue of the pressure of adakite magma genesis has received considerable attention in the literature. As mentioned above, *P* must be high enough to stabilise garnet, but this provides little further constraint. Partial melting experiments on mafic rocks show that the minimum *P* could be anything from slightly less than 1 GPa to 1.6 GPa, depending on the chemistry of the source rock, the temperature and the type of melting reaction involved (e.g. Rapp et al., 1991; Moyen and Stevens, 2005). Some recent experimental work (e.g. Xiong et al., 2005; Xiong, in press) takes the position that rutile must be present, in addition to garnet, in order to explain the negative Ti and Nb anomalies shown by adakitic rocks in multi-element diagrams normalised to primitive-mantle concentrations. This implies magma generation at $P > 1.5$ GPa. However, Foley et al. (2002) presented element-partitioning evidence that they interpret as ruling out eclogitic sources for modern adakites. Furthermore, the partition coefficients for Nb between ilmenite or zircon and melt are up to 50 (Stimac and Hickmott, 1994; Bédard, 2006), suggesting that negative Nb anomalies can have alternative origins, at *P-T* conditions outside those required for rutile stability. The present paper deals with rocks that are, in some important respects, chemically dissimilar to 'normal' adakites. Prior to the present work, very little was known about the conditions of their genesis, or the materials involved, and there is thus no reason to assume that these should be the same as for normal adakites.

The Late Mesozoic granitoids of eastern China occur over wide areas, and lack either temporal or spatial association with subduction (see e.g., summary presented in Xu et al., 2002). These C (continental)-type adakites (Zhang et al., 2001) have all the geochemical attributes of typical subduction-related adakites but, with $K_2O/Na_2O \approx 1$, are distinctly more potassic. These compositional differences must be due either to differences in the source, the physical conditions of magma generation or in the processes that might have modified the compositions of the parent magmas.

Previous experiments on hydrous basaltic rocks show that there are two ways in which relatively potassic, silicic melts can be produced — low degrees of partial melting (<20%) of alkali metabasalt (e.g., Sen and Dunn, 1994) or high degrees of fractionation of hydrous medium- to high-K basaltic magma, especially at high pressures (e.g., Sisson et al., 2005). However, based on the published analyses (e.g., Xu et al., 2002), the Chinese C-type adakites have relatively high K_2O contents and high K_2O/Na_2O over a broad range of SiO_2 contents (~58 to 74 wt.%). The lower part of this SiO_2 range would require much higher *T* (higher-degree) melting or far lower degrees of fractionation from a mafic parent magma. Under such conditions, the melts would no longer be potassic, making such an origin is unlikely. Winther and Newton (1991) and Winther (1996) report on H_2O-undersaturated partial melting experiments on a synthetic low-K tholeiite, at pressures of 0.5 to 3.0 GPa and temperatures of 750 to 1100 °C. The results of their experiments at 900 °C show that melts with higher K_2O contents are produced when the H_2O content of the system is lower (i.e., at lower melt fractions) and when the pressure is higher. For strongly H_2O-undersaturated compositions, their experiments show that K_2O/Na_2O in the melt increases with increasing *P*, from around 0.1 to 0.2 at pressures up to 1.8 GPa to about 0.6 at 3 GPa. The melts are never granitic, always tonalitic or trondhjemitic. Partial melting of some other types of hydrous basaltic rocks at $P > 2.7$ GPa (Rapp and Watson, 1995; Rapp et al., 1999; Skjerlie and Patiño Douce, 2002) can produce melts with K_2O/Na_2O and Al_2O_3 contents that approach those of the Chinese C-type adakites. The implied crustal thicknesses (>90 km) are unrealistically high, however. This led Xu et al. (2002) and Xiao et al. (2004) to hypothesise partial melting of delaminated pods of lower continental mafic crust, deep within the lithosphere. Alternatively, the protoliths for the C-type adakites might not be mafic rocks.

In view of the discussion above, the compositional distinctiveness of Chinese C-type adakites could be due either to a source rock enriched in potassium, the effects of assimilation of metasedimentary rocks in the deep crust (Rapp et al., 2002) or partial melting of mafic crustal rocks at extreme pressures. Isotope studies indicate some crustal involvement, possibly of quite ancient crust (initial $^{87}Sr/^{86}Sr > 0.708$ and $\varepsilon Nd < -13$; e.g., Chen et al., 2002). However, adakites from the Andes, that show isotopic evidence for significant crustal interaction, still have "normal", adakitic K_2O/Na_2O ratios, and significantly lower Rb, Ba, Sr and Pb (LILE) abundances than C-type adakites. Thus, the geochemical peculiarities of C-type adakites must arise from their peculiar potassic source composition, from the particular lower crustal material with which the parent magmas interacted, through very high-*P* melting of ordinary protoliths, or

some combination of these factors. In eastern China there are Early Cretaceous shoshonites and monzonites with high LILE abundances. Their presence suggests a possible "enriched" source for the C-type adakite magmas. Assimilation of metasedimentary (pelitic?) rocks, in the middle to lower crust, could potentially explain the chemistry of these rocks (e.g., McCarthy and Patiño Douce, 1997), provided that the mafic magmas and melts from the metasedimentary rocks remained in effective chemical communication, through diffusion. This may occur in some situations. However, high rates of magma generation, segregation and upward transport through fracture systems (e.g., Clemens and Mawer, 1992; Clemens and Petford, 1999; Petford et al., 2000) are now generally accepted as the rule in felsic magmas. Such rates of magma escape from source regions do not favour assimilation at depth. Indeed, the common worldwide occurrence of large-volume, high-level, felsic, metasediment-derived granitic and volcanic rocks (e.g., Clemens, 2003) suggests that such diffusional exchange is far from a universal occurrence.

The aim of the present work is to use the existing geological and geochemical data on the K-rich adakites, together with new high-*P*-*T* experiments and additional field observations to constrain the models for the genesis of these unusual Chinese adakitic magmas. The results are also of more general interest to those working on the adakite problem. Note that, throughout this paper, we use standard abbreviations for mineral phases (Kretz, 1983).

2. Geology and geochemistry of the Tiantangzhai C-type adakites

C-type (K-rich) adakites have been identified in eastern China (Zhang et al., 2001; Xu et al., 2002) and the Songpan-Garzê Fold Belt (SGFB) of the eastern Tibetan Plateau (Xiao et al., 2006; Zhang et al., 2006; in press). The K-rich adakite starting material used in some of our experiments comes from Tiantangzhai in the Dabieshan Orogen of eastern China (Fig. 1). The Tiantangzhai intrusion is early Cretaceous in age (~130.9±4 Ma, Wang et al., 1998), similar to other C-type adakites in eastern China. The Tiantangzhai porphyritic monzogranites cover an area of about 1300 km^2. They intrude the Neo-Archaean Dabieshan Complex (2.66 Ga, Chen et al., 1996) and are themselves intruded by a medium-grained, aphyric monzogranite dated at 127.9±1.7 Ma (Xu, 2005). The monzogranites are porphyritic in K-feldspar and, locally, some have augen structures and a weak gneissosity. They contain plagioclase (35 to 40 wt%), K-feldspar (25 to 30 wt%), quartz (20 to 30 wt%), biotite (5 to 10 wt%) and minor hornblende, zircon, titanite and ilmenite.

The irregular shape of the outcrop (Fig. 1) and the topography suggest that the exposure may represent the

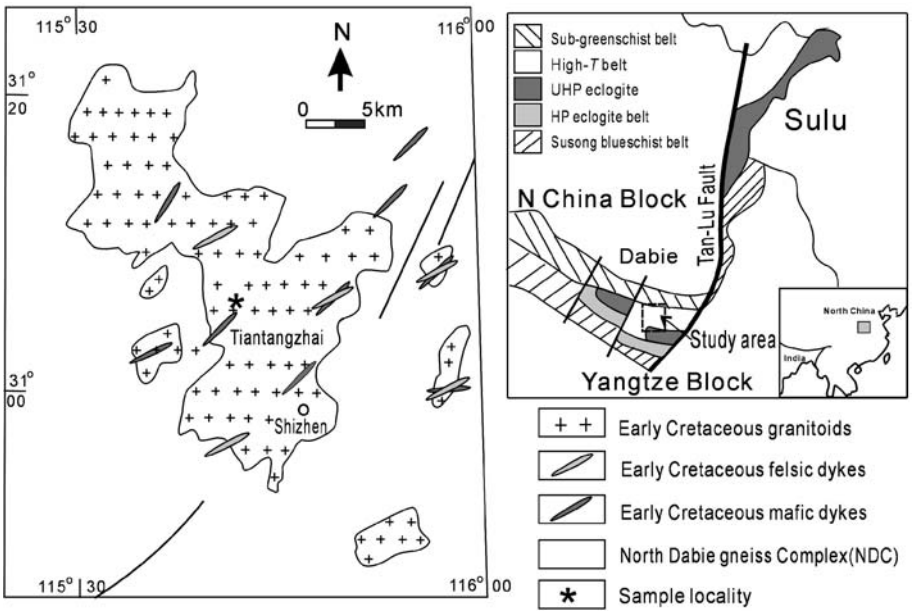


Fig. 1. Simplified geological map showing the location of the study area, within the N China Block, the map of the Tiantangzhai granite and the location from which the K-adakite experimental starting material was taken.

Table 1
Analyses[a] of experimental starting materials (normalised to 100% anhydrous)

	K-adakite 43959	Amphibolite R1617	Shoshonite 98LZ062-1
SiO_2	66.70	57.04	54.22
TiO_2	0.72	0.90	1.07
Al_2O_3	16.64	16.56	17.99
FeO[b]	3.51	8.59	8.03
MnO	0.04	0.17	0.14
MgO	1.00	3.99	4.34
CaO	2.58	7.30	6.61
Na_2O	4.35	4.12	3.44
K_2O	4.18	1.12	3.66
P_2O_5	0.29	0.20	0.50
Original H_2O^+/LOI	0.56	1.18	0.39
Mg#	34	45	49
K_2O/Na_2O	0.96	0.27	1.06
Ni (ppm)	18.32	18	18
Cr (ppm)	36.84	52	12
Sr (ppm)	910.38	89.5	934
Y (ppm)	8.62	11.3	20
Sr/Y	106	8	47
$^{87}Sr/^{86}Sr_{132}$	0.708048		
εNd_{132}	−18.7		

[a] Data for 43959, R1617 and 98LZ062-1 from Xu (2005), Yan (2005), and Wang et al. (2006), respectively.
[b] Total Fe as FeO.

roof zone of a pluton up to 49 km long and 29 km wide. If we apply the general relationship found by McCaffrey and Petford (1997) between pluton diameter and thickness, the Tiantangzhai mass probably has a total thickness of around 3 km. We can estimate the emplacement depth using the experimentally calibrated Al-in-hornblende barometer of Anderson and Smith (1995). Wang et al. (2000) gave 6 analyses of the hornblendes (all very similar) from the Tiantangzhai monzogranite. Averaging these, we calculate $Al_{tot}=1.398$, using a formula unit with $23O^{2-}$. The barometer then yields 264±60 MPa for the emplacement pressure, or about 10 km depth, assuming a temperature of 750 °C for the crystallisation of hornblende (consistent with its texturally late appearance in the crystallisation sequence).

The Neo-Archaean Dabie Complex country rocks are dominated by metamorphosed TTG-series rocks (Tonalites, Trondhjemites and Granodiorites). An extensive migmatite zone, with widths varying from a few meters to a few tens meters, is developed along the contact with the intrusion. Country rocks further away from the intrusion experienced less migmatisation and are intruded by scarce, narrow (<1 m), irregular monzogranite dykes. Our additional observations are given later.

Geochemical and isotopic studies of the Tiantangzhai monzogranites have been carried out by Ma et al. (1998), Wei et al. (2001), and Xu (2005). The data show that the porphyritic monzogranite has adakitic affinities but the medium-grained monzogranite has the characteristics of a normal I-type granite (Xu, 2005). Sample 43959 (used in the experimental study) was taken from the central part of the Tiantangzhai porphyritic monzogranite (N 31° 05′ 25.8″, E 115° 47′ 27.5″). It is fresh, with minimal alteration and no foliation or migmatisation. Its major-element, REE and Sr–Nd isotope chemistry are given in Table 1 and illustrated in Fig. 2. The rock has high total alkalis ($K_2O+Na_2O=8.53$ wt%) and K_2O/Na_2O (0.96). It belongs to the high-K calcalkaline series, has a very high Sr/Y ratio (106), no Eu anomaly and strong depletion HREE, indicating the presence of garnet, but without plagioclase, in the residue. Published REE partition coefficients for hornblende and plagioclase (summarised in Rollinson, 1993) suggest that the presence of a large amount of hornblende as a residual mineral in the magma source could negate the influence of a small amount of residual plagioclase, producing a melt lacking a negative Eu anomaly. However, Rapp and Watson (1995) showed that fluid-absent partial melting of metabasic rocks only produces adakitic liquids (and melts of any significant quantity) at temperatures above amphibole stability. Thus, we infer that large amounts of residual hornblende are most unlikely to have been present. The observed lack of a Eu anomaly is best interpreted as indicating the absence of residual plagioclase. The Tiantangzhai monzogranite has relatively high ($^{87}Sr/^{86}Sr)_i=0.708048$ and very low $\varepsilon Nd(t)=-18.7$, suggesting a very ancient igneous source rock. This sample has geochemical features similar to adakites (as defined by Defant and Drummond, 1990), with the

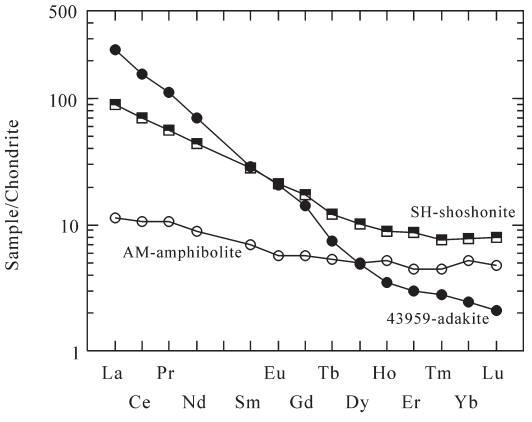


Fig. 2. Chondrite-normalised REE patters for adakite, amphibolite and shoshonite starting materials (data sources as in Table 1).

exception of its high K_2O content, and is typical of the widespread C-type adakites in eastern China.

3. Experimental evidence

3.1. Starting materials

Two types of experiments were carried out. The first were near-liquidus runs on an intrusive K-adakite. The second series were fluid-absent partial melting experiments on a quartz tholeiitic amphibolite (R1617) and a shoshonite (98LZ062-1), both from the Dabieshan area. The amphibolite has a mode of 42% Pl, 38% Hbl, 13% Qtz, 5% Bt and 2% phengitic muscovite. The shoshonite contains Pl, Cpx, Kfs and minor Bt, Hbl and Qtz. Table 1 shows the major-element, selected trace-element and, where available, the isotopic analyses of the three starting materials.

The K-rich adakite sample 43959 is from the Tiantangzhai granite. It was chosen as the starting material because this rock is typical of K-rich adakites from eastern China, in terms of its geochemistry, isotope characteristics and age (130 Ma) corresponding to the Yangshanian orogeny. Its petrology and geochemistry are well documented (Ma et al., 1998; Wei et al., 2001; Xu, 2005), as summarised above. The pluton is located within the well known Dabieshan UHP metamorphic belt (formed at 220 to 240 Ma), and is a manifestation of the widespread and voluminous post-collisional magmatism in this area. The chosen sample is mineralogically and chemically representative of the rocks that form the bulk of the intrusion and we therefore infer it to be similar in composition to the parent magma. It could be suggested that K-rich magmas, such as the Tiantangzhai granite, could be produced through assimilation of crustal rocks by a mantle-derived mafic magma. Assimilants such as tonalites and trondhjemites are unsuitable, as none of these are sufficiently rich in K_2O. The most feasible assimilants would be pelites and greywackes. We performed a variety of calculations, starting with a potassic Karoo olivine tholeiite and assimilating an average post-Archaean shale (Taylor and McLennan, 1985). Using such end members, no bulk assimilation or AFC model can simultaneously explain the SiO_2 content, Mg# (100Mg/[Mg+Fe]) and K_2O/Na_2O of the K-rich adakites. The same is true for mixing between the basalt and potassic, metasediment-derived partial melts (e.g. LeBreton and Thompson, 1988). To reach the required SiO_2 content (~67 wt%) would require mixing with >60 wt% of metapelite melt, leaving the hybrid magma with K_2O/Na_2O and Mg# far too high. Furthermore, the Tiantangzhai pluton shows no field evidence of magma mixing and mingling (e.g., synplutonic mafic dykes or mafic magmatic enclaves) or direct spatial association with mafic intrusions. We thus infer an origin by crustal melting. Experiments on our starting material should therefore produce valid constraints on the conditions of magma generation.

3.2. Run conditions and experimental strategy

The philosophy behind the near-liquidus experiments is that, at the pressure and temperature at which a magma is generated, the melt will be in equilibrium with the mineral phases that constitute the restite. If the magma then remained near its site of generation and crystallised, the near-liquidus phases would mimic the phases in the restite. Thus, a series of experiments were carried out, with the aim of locating the liquidus, at reasonable melt H_2O contents (2, 4 and 6 wt.% H_2O), with the added constraint that the near-liquidus phases should include garnet but not plagioclase. The presence of garnet was inferred from the HREE-depleted signature of the Chinese K-rich adakites (including the starting material). The absence of plagioclase was inferred from the lack of a negative Eu anomaly in the REE spectra, and the Sr/Y ratio. At appropriate P, T and melt H_2O content, these experiments provide two things — estimates of the conditions of formation of the K-rich adakite magmas and constraints on the mineral assemblage of the restite. The optimum conditions, determined from these experiments, were then used for the experimental P and T of the fluid-absent partial melting experiments.

The idea behind the partial melting experiments is that granitic magmas, such as the K-rich adakites, are markedly H_2O-undersaturated, and formed by fluid-absent partial melting of crustal materials. This scenario has been shown to be the case for the great majority of high-level, high-temperature granitic magmas, worldwide, where the magmas are dominated by the crustal contribution (Clemens and Watkins, 2001). The results of these experiments are used to constrain the types of crustal source materials that could have been involved in the genesis of the K-rich adakite magmas. Criteria for the suitability of a potential source rock are: first that the restitic phases present at the P and T inferred for magma generation are similar to those found near the liquidus of the adakite, and second that the composition of the melt formed in the experiments mimics that of the K-rich adakite itself.

3.3. Experimental methods

Starting rocks were ground, in agate ball mills, until their grain size was <5 μm. The samples were then dried at 110 °C and stored in a vacuum desiccator over silica

gel. Gold was chosen as the capsule material because it is far better than Pt and Pd alloys with respect to its propensity to absorb Fe from the sample (increasing Mg#). Additionally, Au is far less permeable to H_2 than Pt or Pd alloys, and therefore retards loss or gain of H_2 in the samples, approximately maintaining fO_2 at whatever level results from internal control by equilibria in the sample.

For each experiment, one end of an annealed Au capsule (3 mm OD, 0.15 mm wall thickness) was sealed, by arc welding, and approximately 0.015 g of starting material was placed inside and gently compacted. Fluid-absent capsules (shoshonite and amphibolite partial melting experiments) were then placed inside a drying oven at 110 °C for at least 30 min and finally sealed by carbon arc welding. For near-liquidus experiments on the C-type adakite, the amount of added starting material was accurately weighed and then small measured quantities of distilled, deionised H_2O were added, by microsyringe, prior to sealing. To cool the capsules during welding and prevent H_2O loss, we used a steel heat sink (thin vice jaws) at the top of the capsule, just below the weld, and wet tissue paper wrapped around the rest of the capsule. In some cases, capsule weights could be re-measured, after sealing, to check for potential volatile loss; none was detected. However, for many capsules, there were small losses of capsule metal, due to sputter from the weld, rendering such checks impossible. Nevertheless, the available evidence suggests that the cooling technique was effective in retaining the H_2O in the capsules. The total H_2O contents of the charges were then calculated from the H_2O content of the starting rock (OH^- in hydrous minerals) plus the added H_2O. The total H_2O contents in three series of runs were approximately 2, 3.7 and 6 wt%. During the runs, all the H_2O was dissolved into the melt and the experiments were therefore fluid-absent (strictly classified as fluid-deficient experiments).

Experiments were carried out in a 12.7 mm diameter, non-end-loaded, piston-cylinder apparatus (Depths of the Earth Company, Cave Creek, Arizona, USA) at Kingston University. All the experiments were at $T \geq 900$ °C, so we used NaCl-borosilicate glass cells. We used boron nitride (BN) packing around the capsules, to minimise H_2 loss (Truckenbrodt et al., 1997) and the associated increase in fO_2 and decrease in aH_2O. Thermocouples were type-K (chromel-alumel). The distance between the thermocouple and the sample capsule was minimised (0.5 mm, the thickness of the alumina disc) to prevent T uncertainties due to thermal gradients within the cells. Temperatures are nominally accurate to ±1 °C. Precision in pressure control varied between different experiments but was generally around ±0.02 GPa.

The cylinder was lightly lubricated with molybdenum disulphide grease before the sample assembly (wrapped in Pb foil) was inserted. Before switching on the furnace, the whole assembly was pressurised to final run pressure. Experiments all had a fifteen-minute ramp-up time to reach their final T, while P was maintained at the desired final value. Run durations were between 25 and 72 h. These run durations were based on our own previous experience of what is necessary to obtain near-equilibrium conditions and crystal growth to a reasonable size for analysis. Duplicate runs were carried out at 2 GPa and 1000 °C — one of 50 h and another of 66 h duration. The changes in phase proportions and compositions were small. The only apparent difference in assemblage is that the slight trace of Kfs in the product of the shorter run was not present in the product of the longer run. Solid products are all quite similar in chemistry, although the melt did evolve chemically. We subsequently settled on 66 h as our standard run duration. Based on previous studies of the redox conditions in this piston-cylinder apparatus, $\log fO_2$ is believed to lie between QFM and QFM-2 (Graphchikov et al., 1999).

Experiments were terminated by switching off the furnace while maintaining constant pressure until the solidus temperature was reached. This prevented vesiculation of any glass present, due to the exsolution of volatiles. The quenches took a few seconds. Quench crystallisation was not encountered in these types of experiments, with relatively viscous melts and rapid quench times.

When the runs were completed, the capsules were removed from the cells, cleaned, opened and the contents examined. It was not feasible to measure post-run capsule weight because of the degree of deformation of the capsules, pressure cell materials adhering to folds in the metal and small losses of capsule metal into the furnace and pressure cell during the run. Nevertheless the state of the samples (lack of oxidation and colour zoning, presence of abundant glass, etc.) suggested that the capsules had remained intact in all experiments reported here. Most of each sample was ground by hand in an agate mortar and a grain mount made, for examination with an optical microscope. A single larger piece of each run product was mounted in epoxy resin, sectioned and polished for analysis with the SEM/microprobe.

3.4. Analytical methods

The SEM/probe was used to make/confirm phase identifications, and to obtain analyses of the crystalline phases present. However, this is of secondary importance

Table 2
Results of experiments

Run No	Starting material	Sample mass (g)	H_2O added (g)	Total H_2O (wt%)	P (GPa)	T (°C)	Durn (h)	Products[a]	Comments
Near-liquidus runs									
KADAK-1	43959	0.01575	0.00023	1.99	1.993±0.016	950±1	25	(gl), Qtz, Afs, Pl, (Bt), (Omp) Grt	2fsp=sanidine Or_{54} and An_{21}
KADAK-14	43959	0.01556	0.00050	3.66	1.507±0.025	1025±1	40	gl, Afs, Pl, Cpx, Opx, (Ap)	2fsp=anorthoclase Or_{22} & An_{20}
KADAK-15	43959	0.01532	0.00050	3.70	1.706±0.030	1025±1	67	gl, Pl, Cpx, Opx, Grt, (Ru, Ilm)	Pl=An_{17}
KADAK-2	43959	0.01495	0.00049	3.72	2.028±0.017	900±1	41	gl, Qtz, Pl, Afs, (Bt), Omp, (Grt)	2fsp=sanidine Or_{67} & An_{21}
KADAK-4	43959	0.01571	0.00049	3.57	2.020±0.018	950±1	64	gl,(Qtz),Pl, Afs, Omp, Grt, (Ru, Ap)	2fsp=sanidine Or_{59} & An_{20}
KADAK-9	43959	0.01552	0.00050	3.66	1.999±0.035	975±1	65	gl, Pl, Afs, Cpx, Grt	sanidine Or_{53}
KADAK-6	43959	0.01557	0.00050	3.65	2.019±0.020	1000±1	50	gl, Pl, (Afs), Omp, Grt, (Ap, Ru?)	2fsp=anorthoclase Or_{28} & An_{17}
KADAK-7	43959	0.01512	0.00048	3.62	2.011±0.034	1000±1	66	gl, Pl, Omp, Grt, (Ru)	Pl=An_{19}
KADAK-8	43959	0.01542	0.00050	3.68	2.010±0.021	1025±1	69	gl, Pl, Omp, Grt, (Zrn, Ru, Ap)	Pl=An_{18}
KADAK-12	43959	0.01523	0.00050	3.72	2.007±0.014	1050±1	65	gl, Pl, Afs, Omp, Grt	2fsp=sanidine Or_{43} & An_{17}
KADAK-19	43959	0.01561	0.00050	3.65	1.997±0.011	1075±1	66	gl, Pl, Omp, (Opx), Grt, (Ru, Ap)	Pl=An_{24}
KADAK-11	43959	0.01567	0.00050	3.63	2.502±0.019	1000±1	65	gl, Qtz, Afs, Omp, Grt, (Ru)	fsp=sanidine ~ Or_{42}
KADAK-16	43959	0.01521	0.00090	6.12	1.722±0.031	1050±1	68	gl, Cpx, (Opx), (Ap)	
KADAK-10	43959	0.01502	0.00088	6.06	2.011±0.019	975±1	65	gl, Afs, Pl, Omp, Grt, (Ru, Ap)	2fsp=anorthoclase Or_{24} & An_{12}
KADAK-13	43959	0.01566	0.00090	5.96	2.010±0.028	1025±1	66	gl, (Pl), Cpx, Grt	
KADAK-18	43959	0.01562	0.00090	5.98	2.027±0.020	1050±1	66	gl, Cpx, (Opx?), (Ap)	
KADAK-21	43959	0.01532	0.00090	6.08	2.526±0.023	1050±1	67	gl, Cpx?, Grt, (Ru)	
KADAK-22	43959	0.01514	0.00090	6.14	2.510±0.015	1075±1	66	gl, (Omp, Grt)	very close to liquidus
Fluid-absent partial melting runs									
SH-1	98LZ062-1		–	0.40	1.512±0.019	1050±1	77	gl, Pl, Cpx, Grt, (Ap)	
SH-2	98LZ062-2		–	0.40	2.028±0.024	1050±1	68	gl, (Pl), Cpx, Grt, (Ru?, Ap)	Cpx=Jd_{20}
SH-3	98LZ062-2		–	0.40	2.489±0.015	1075±1	116	(gl), Omp, Grt, (Ru, Ap)	
AM-1	R1617		–	1.19	2.031±0.027	950±1	70	(gl), Omp, Grt, (Ru)	
AM-2	R1617		–	1.19	~ 2	1050±1	30	gl, Omp, Grt	
AM-3	R1617		–	1.19	2.520±0.025	1075±1	89	(gl), Omp, Grt, (Ru, Ap, Zrn)	

Afs=alkali feldspar (anorthoclase or sodic sanidine).
Cpx=augitic clinopyroxene (Jd≤20 mol%).
Omp=omphacitic clinopyroxene (Jd>20 mol%).
( )=minor to trace quantity of phase.
[a] Standard mineral abbreviations of Kretz (1983), with the addition of gl=glass.

to the compositions of the glasses in the products of the partial melting experiments, as we are trying to match these with natural K-rich adakite compositions. The fairly small sizes of the melt pockets produced in the fluid-absent partial melting runs limited the sizes of the rastered areas that we could analyse. This technique of rastering the electron beam over the sample was used to minimise the well documented counting losses on Na, during analysis of hydrous glasses.

All analyses were carried out using the JEOL 3200 SEM, fitted with an Oxford Instruments ISIS EDS system, at Kingston University. The tiny chips of

Table 3
Analyses of crystalline phases (normalised to 100% anhydrous) formed in some critical experiments

Phase (No of analyses)	Pl (4)	Grt (3)	Grt (4)	Grt	Grt	Px (2)	Px (7)	Px (8)	Px (6)
Run No	KADAK-19	KADAK-19	KADAK-22	SH-3 (10)	AM-3 (5)	KADAK-19	KADAK-22	SH-3	AM-3
P (GPa)	2	2	2.5	2	2.5	2	2.5	2.5	2.5
T (°C)	1075	1075	1075	1075	1075	1075	1075	1075	1075
H_2O (wt%)	3.7	3.7	6	–	–	3.7	6	–	–
SiO_2	62.75	38.35	39.89	37.30	37.85	50.54	52.88	51.93	51.22
TiO_2	n.a.	2.09	1.20	2.46	1.12	1.40	1.07	1.26	1.22
Al_2O_3	24.07	20.35	20.72	19.45	20.04	10.64	8.58	9.46	9.81
FeO*	n.a.	24.84	20.12	24.79	25.62	10.24	4.41	10.17	10.74
MnO	n.a.	0.45	0.61	0.62	0.50	n.a.	0.13	0.09	0.17
MgO	n.a.	7.48	9.55	6.11	5.31	10.09	11.56	8.03	8.23
CaO	4.64	6.45	7.91	9.26	9.56	14.08	17.85	15.17	14.40
Na_2O	6.93	n.a.	n.a.	n.a.	n.a.	2.90	3.53	3.89	4.21
K_2O	1.60	n.a.	n.a.	n.a.	n.a.	n.a.	n.a.	n.a.	n.a.
original total	92.76	99.71	97.86	99.54	98.10	99.40	99.10	98.84	99.15
structural formula†	8 O^{2-}	12 O^{2-}	12 O^{2-}	12 O^{2-}	12 O^{2-}	6 O^{2-}	6 O^{2-}	6 O^{2-}	6 O^{2-}
Si	2.777	2.962	3.017	2.910	2.959	1.862	1.909	1.917	1.885
Ti		0.121	0.068	0.144	0.066	0.039	0.029	0.035	0.034
Al^{iv}	1.256	0.038	0.000	0.090	0.041	0.138	0.091	0.083	0.115
Al^{vi}		1.818	1.852	1.708	1.814	0.324	0.274	0.328	0.310
Fe^{3+}		0.053	0.055	0.130	0.107	0.000	0.005	0.000	0.036
Fe^{2+}		1.551	1.217	1.488	1.568	0.317	0.128	0.314	0.294
Mn		0.029	0.039	0.041	0.033		0.004	0.003	0.005
Mg		0.861	1.077	0.711	0.619	0.554	0.622	0.442	0.452
Ca	0.220	0.534	0.641	0.774	0.801	0.556	0.690	0.600	0.568
Na	0.595					0.207	0.247	0.278	0.300
K	0.090								
cation total	4.938	7.968	7.967	7.996	8.007	3.995	3.999	4.000	4.000
Mg#		36	47	32	28	64	83	58	61
composition	An_{24}	Pyp_{30}	Pyp_{36}	Pyp_{24}	Pyp_{20}	Jd_{21}	Jd_{25}	Jd_{28}	Jd_{30}

* total Fe as FeO.
† ferric iron contents calculated using the method of Droop (1987).

experimental run products, mounted on glass slides, did not always take a perfectly flat, level polish. The effect of this was either too great or too little absorption of emitted X-rays, depending on the angle of the surface slope relative to the collector. The analytical totals therefore commonly depart from the ideal. However, the stoichiometry of the crystalline phases does not appear to be greatly affected, and the mineral analyses are sufficiently accurate for calculation of parameters such as Mg# and end-member proportions in pyroxenes, garnets and feldspars. Patches of glass (quenched melt) were relatively small in the partial melting experiments (AM and SH runs). To minimise counting losses on light elements (mainly Na) these were analysed using a static broad beam technique that maximised the area analysed, for a given glass patch. As is usual with hydrous glasses, the analytical totals fell well below ideal values. This reflects reduced X-ray yields from such materials, and the totals are essentially meaningless unless calibrated against a series of hydrous glasses of similar silicate composition (see e.g., Devine et al., 1995). Since we were unable to apply such corrections, all glass analyses are reported normalised to 100 wt% anhydrous.

3.5. Results of experiments

There were 18 successful near-liquidus and 6 partial melting experiments. The details of these runs are given in Table 2, which shows the total H_2O contents of the experimental charges, temperatures, pressures and durations of the runs, as well as the phases present in the run products. Table 3 shows analyses of solid phases from some of the critical experiments and Table 4 shows the compositions of the glasses (quenched melts) in the experiments of Table 3. The complete set of average analyses of run products can be obtained from the authors, upon request.

3.5.1. K-rich adakite near-liquidus runs

This series of experiments was designed to locate the liquidus of the K-rich adakite starting material. The first run, with ~2 wt% H_2O was carried out at 2 GPa and

Table 4
Analyses[a] of glasses (normalised to 100% anhydrous) formed in partial melting experiments

	SH1 1.5 GPa 1050 °C $n=4$	SH2 2.0 GPa 1050 °C $n=3$	SH3 2.5 GPa 1075 °C $n=6$	AM1 2.0 GPa 950 °C $n=3$	AM3 2.5 GPa 1075 °C $n=3$
SiO_2	61.99 (0.21)	62.57 (0.14)	64.06 (0.76)	72.45 (1.63)	66.83 (0.78)
TiO_2	0.78 (0.18)	0.90 (0.17)	0.85 (0.22)	0.41 (0.36)	1.26 (0.20)
Al_2O_3	19.62 (0.16)	19.64 (0.48)	18.88 (0.34)	17.39 (0.42)	16.55 (0.42)
FeO[b]	2.88 (0.25)	1.79 (0.11)	2.09 (0.44)	2.20 (0.32)	4.58 (0.53)
MnO	0.08 (0.06)	0.09 (0.07)	0.07 (0.07)	n. a.	0.06 (0.05)
MgO	0.75 (0.08)	0.67 (0.14)	0.77 (0.27)	0.67 (0.57)	0.91 (0.10)
CaO	2.02 (0.05)	1.47 (0.11)	1.61 (0.31)	1.80 (1.15)	2.26 (0.28)
Na_2O	5.50 (0.15)	6.01 (0.02)	4.73 (0.34)	3.10 (0.22)	4.48 (0.29)
K_2O	6.29 (0.10)	6.77 (0.10)	6.86 (0.29)	1.97 (0.16)	2.19 (0.05)
P_2O_5	0.09 (0.11)	0.10 (0.17)	0.08 (0.15)	n. a.	0.81 (0.11)
K_2O/Na_2O	1.14	1.13	1.45	0.64	0.49
Mg#	32	40	40	35	27
A/CNK	1.00	0.99	1.04	1.66	1.20

[a] mean (standard deviation), n=number of analyses.
[b] total Fe as FeO.

950 °C. The products included abundant crystalline material (~80%), with two feldspars, quartz and biotite, in addition to garnet. It was thus clear that such a low H_2O content was inappropriate. Indeed, most granitic magmas that formed at $T>800$ °C have initial H_2O contents around 4 to 6 wt% (e.g., Scaillet et al., 1998). Consequently, a series of experiments was carried out with ~3.7 wt% H_2O, at pressures ranging from 1.5 to 2.5 GPa. Note that, with proximity to the liquidus, the melt present in a run would have an H_2O content very close to the H_2O in the experimental charge, as listed in Table 2, since the melt is the only hydrous phase present. It became apparent that, in order to approach the liquidus at this H_2O content, very high temperatures would be required, and experiments were therefore conducted at T up to 1075 °C. However, at none of the conditions investigated were we able to find a near-liquidus assemblage without feldspar (plagioclase or alkali feldspar), as required by the trace-element chemistry of the K-rich adakites. In addition, the experiments, even at 1075 °C, were not sufficiently close to the liquidus. All had crystal contents of tens of percent. Finally, we carried out several experiments with ~6 wt% H_2O, and succeeded in locating experimental conditions very close to the liquidus, with only traces of garnet and clinopyroxene present, in addition to the melt. This final near-liquidus experiment (KADAK 22, Table 2) was at 2.5 GPa and 1075 °C. Fig. 3 shows the textures and phases present in a selection of the run products from the near-liquidus experiments.

Average analyses of the major crystalline phases in two of the important experimental runs are given in Table 3. KADAK-19 (at 2 GPa and 1075 °C) contains sodic plagioclase (~An_{24}), almandine-rich, low-grossular garnet (Pyp_{30}) and magnesian clinopyroxene with an Na_2O content that places it just into the omphacitic group (Jd_{21}). In KADAK-22 (at 2.5 GPa and 1075 °C) there is no plagioclase, the garnet is a little more magnesian (Pyp_{36}) and the pyroxene is more highly magnesian, with a higher Na_2O content, making it definitely omphacitic (Jd_{25}). In this series of experiments the pyroxene compositions evolve from sodic aluminous augites at $P<2$ GPa, through slightly omphacitic compositions at 2 GPa, to true omphacites at $P>2$ GPa.

On the basis of these results, we suggest that the K-rich adakite magma, though very H_2O-undersaturated, must have been quite hydrous and that, if 6 wt% is a reasonable estimate of the initial H_2O content, the initial temperature must have been around 1080 °C. Furthermore, the pressure of generation must have been >2 GPa, possibly near 2.5 GPa. Thus, contrary to our initial expectations, the magma was very hot, rather wet and formed deeper in the lithosphere that had been previously been thought.

In view of the above results, the final partial melting experiments were carried out at 2.5 GPa and 1075 °C. Fig. 4 shows some of the run products. We did not perform experiments at higher T because we did not wish to approach the melting point of the gold capsules too closely. Already at 1075 °C, the gold was flowing laterally and, at the corners of the capsules, beginning to form feathery intrusions into the graphite furnace. Despite its desirability as a capsule material that minimises Fe-alloying and H_2 migration, we were clearly carrying out experiments near the limits of gold's mechanical suitability.

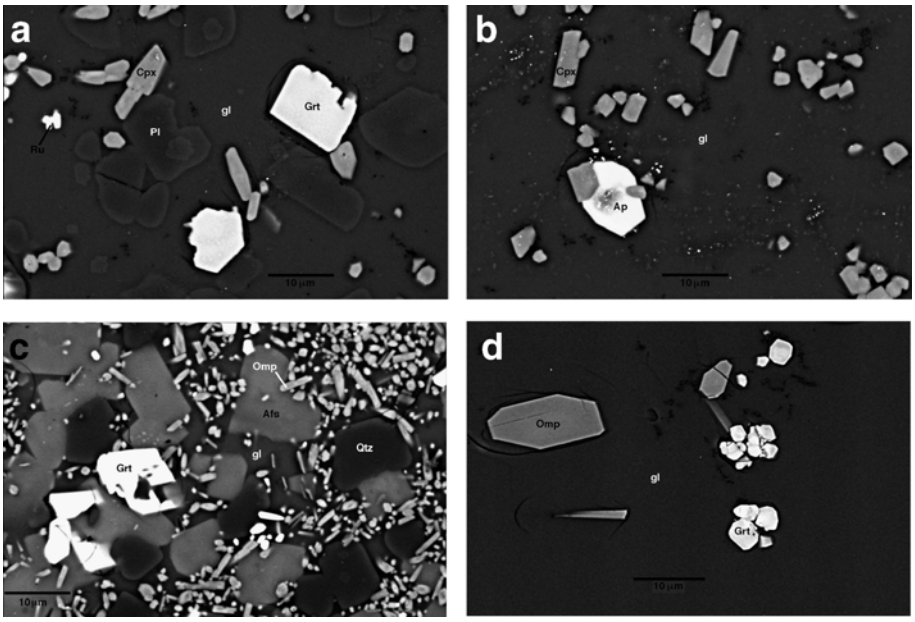


Fig. 3. SEM backscattered electron images of the products of some of the near-liquidus experiments on K-adakite 43959. All images are at the same magnification, with scale bars of 10 μm shown. a. KADAK-19 with 3.6 wt% H_2O at 2 GPa and 1075 °C. This run product contains the required Grt but also has Pl in abundance. Note also that, at this H_2O content, the crystal content is still substantial, ~50%. b. KADAK-18 with 6 wt% H_2O at 2 GPa and 1050 °C is much closer to the liquidus (~25% crystals) and free of Pl but contains no Grt either. The bright phase is apatite. c. KADAK-11 with 3.63 wt% H_2O at 2.5 GPa and 1000 °C is at far too low a *T* and contains a large percentage of crystals (~90%), including both Qtz and Afs. Note, however, that Pl is absent at this high *P*, having been supplanted by omphacitic clinopyroxene. d. KADAK-22 with 6 wt% H_2O at 2.5 GPa and 1075 °C is very close to the liquidus (~5% crystals), with only a small proportion of Omp and Grt present — residual phases compatible with the formation of a melt with HREE depletion and lacking a Eu anomaly.

3.5.2. Amphibolite melting

The results of the three experiments on this starting material are shown in Table 2. Two were carried out at 2 GPa, and the final one at 2.5 GPa. Note also that experiment AM2 (at 2 GPa and 1050 °C) is suspect, due to a pressure drop during the run (occasioned by partial failure of the tungsten carbide core of the vessel). Thus, the results of AM2 should only be taken as indicative. In addition, the melt pools in AM2 were too small to analyse without contamination from surrounding crystals. The more important experiment is AM3, carried out near the conditions inferred for the liquidus of the K-rich adakite starting material. Results show peraluminous tonalitic (dacitic) glass (Table 4) coexisting with almandine-rich garnet (Pyp_{20}), omphacitic pyroxene (Jd_{30}) and accessory Ru, Ap and Zrn (Fig 4b). The peraluminous melt chemistry may seem unusual but Patiño Douce and Beard (1995) produced peraluminous granodioritic melts by fluid-absent partial melting of a synthetic quartz amphibolite. Thompson and Ellis (1994) also produced felsic peraluminous melts through fluid-absent partial melting, involving breakdown of aluminous hornblende, at $P>1.5$ GPa, in model amphibolites in the CMASH system. It seems clear that low-degree partial melts of certain types of mafic to intermediate amphibolitic rocks, at high pressures, are indeed peraluminous. Much higher-degree, wet basalt melting also produces peraluminous liquids at temperatures up to the amphibole-out phase boundary (e.g., Rapp, 1995). The formation of peraluminous melts from metaluminous protoliths (or magmas) by extraction of amphibole or clinopyroxene is a process that has been recognised for many decades (e.g., Kushiro and Yoder, 1972; Cawthorn and O'Hara, 1976; Abbott, 1981). The general features of the chemistry of the melt formed in AM3 are similar to those of the K-rich adakite. However, although the K_2O/Na_2O of the experimental melts was clearly higher than that in the starting material (0.27, Table 1), the values did not closely approach those typical of K-rich adakites (~1), remaining instead below 0.65. In addition, the melts were highly peraluminous, a feature not encountered among adakitic rocks.

3.5.3. Shoshonite melting

There were also three experiments carried out on this starting material, ranging in *P* from 1.5 to 2.5 GPa. All melts formed were olivine-normative and syenitic. The important experiment is SH3 (Fig. 4d), carried out at the *P-T* conditions for K-rich adakite genesis, as inferred

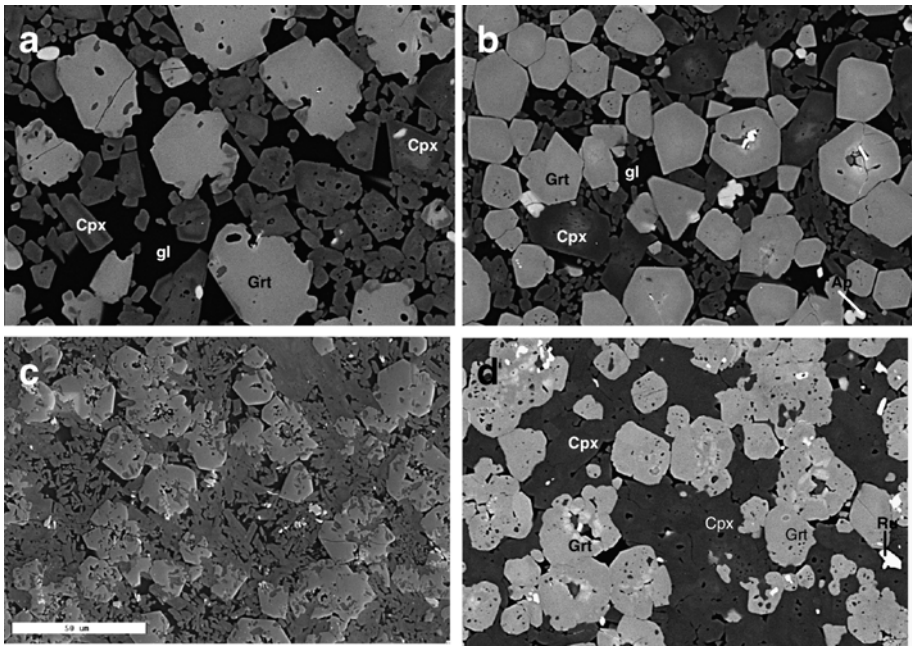


Fig. 4. SEM backscattered electron images of the products of the fluid-absent partial melting experiments. a. shoshonite run SH-1 at 1.5 GPa and 1050 °C, showing an assemblage of Pl+Cpx+Grt. b. shoshonite run SH-3 at 2.5 GPa and 1075 °C, showing a small amount of glass (quenched melt) coexisting with Grt and Omp. c. amphibolite run AM-1 at 2 GPa and 950 °C showing glass coexisting with Cpx and Grt. d. amphibolite run AM-3 at 2.5 GPa and 1075 °C showing glass coexisting with Omp and Grt. Note that both starting materials produced melts coexisting with omphacitic pyroxene and garnet similar in composition to the near-liquidus phases formed in experiment KADAK-22 (see Table 3).

from the near-liquidus K-adakite experiments. Here, weakly peraluminous syenitic (trachytic) glass (with 64 wt% SiO_2, $K_2O/Na_2O=1.46$ and Mg#=40) coexists with almandine-rich garnet, sodic aluminous augite and accessory Ru and Ap. The cores of the garnets are slightly more almandine-rich than the rims, which are slightly richer in grossular and pyrope components. The bulk of the pyroxene in SH3 is small- to medium-sized crystals of omphacite (Jd_{28}). There are also a few larger, zoned pyroxene crystals in which the cores are relatively Fe-enriched, aluminous, sodic augite (Jd_{11}) and the rims are more magnesian omphacite (Jd_{35}). All these pyroxenes were formed during the run, so this represents a small degree of disequilibrium.

4. Field observations

The results of the near-liquidus experiments on the K-rich adakite suggest that the magma was substantially hotter (>1050 and probably >1075 °C) than normally inferred for monzogranites and granodiorites (≤900 °C). We therefore examined this pluton in the field, to determine whether there is evidence for unusually high-*T* or a wide thermal aureole.

The country rocks around the Tiantangzhai granite are TTG rocks that were metamorphosed to granulite facies at about 2.6 Ga (Chen et al., 1996). In such felsic rocks, with these metamorphic assemblages, it is difficult to discover the true width or grade of any thermal aureole that might be present. However, there are features of the aureole that support a high temperature of intrusion. As suggested above, there are migmatites at the contact with the country rocks. We examined the margin of the pluton in its north-western sector. Remote from the granite, the TTG rocks have a very consistent planar fabric, with quite regular alternations of light and dark layers on a scale of about 5 mm. However, within 300 m of the intrusion, the rocks are comprehensively retrogressed to amphibolite facies and the regular planar fabric begins to show signs of fracturing and slight rotation of blocks, accompanied by the presence of small, cross-cutting strings and pods of leucocratic rock with an igneous texture. The pods have distinct melanosomes rich in biotite. These features suggest retrogression of the country rocks through the thermal effects of the intrusion, coupled with permeation by fluids evolved from the cooling and solidifying magma. At this distance, the leucocratic pods appear to be melts injected, into the deforming country rock, from partially melted migmatitic sources closer to the intrusion. This could be termed an injection migmatite. The migmatisation becomes more intense as the pluton

is approached, and the rocks become metatexites, in which the melts seem to be locally derived. At a distance of about 80 m from the pluton, the TTG wall rocks are diatexites that contain enclaves of the more mafic (less melted) layers in the protolith (e.g., Fig. 5).

There are many examples in the literature of syn-metamorphic plutons that caused contact anatexis in terranes already undergoing high-grade regional metamorphism (e.g., Powers and Bohlen, 1985; Finger and Clemens, 1995). The difference here is that there was no such regional metamorphic event (at least at the level of granite emplacement). Thus, the partial melting and migmatisation around the Tiantangzhai granite must be entirely due to the high T of intrusion, probably aided by the flux of aqueous fluids from the crystallising magma (c.f., the Ballachulish aureole in Scotland; Holness and Clemens, 1999; Clemens and Holness, 2000).

The fluid-present character of the migmatisation is evident from the mineralogy of the mesosome and melanosome, both of which contain biotite, with no sign of pyroxene or, most importantly, its pseudomorphs (see e.g., Clemens and Droop, 1998). Thus, partial melting occurred under amphibolite- or hornblende hornfels-facies conditions, consistent with the inferred emplacement pressure of 260 MPa (around 10 km depth).

Another field observation relevant to the genesis of the granite is that the pluton seems to contain only xenoliths of the TTG country rock. There are apparently no enclaves of mingled mafic magma. Thus, either any juvenile additions of mantle-derived magma must have been deep-seated (near-source), or there were no such additions.



Fig. 5. Field photograph of migmatised (partially melted) TTG country rock close to the margin of the Tiantangzhai granite. The coin is a 1 Yuan piece, about 2 cm in diameter. Note the generally diatexitic fabric and the development of cross-cutting granitic leucosomes that separate portions of the more mafic (refractory) layers.

To illustrate the requirement for the Tiantangzhai magma to have been at a temperature higher than normally associated with granitic intrusions, we carried out two-dimensional thermal modelling using the 1995 revision of the HEAT3D software package (Wohlerz and Heiken, 1991). We assumed that thermally isotropic country rocks had a density $\rho = 2700$ kg/m^3, heat capacity Cp = 890 J/kgK and thermal conductivity $k = 2.5$ W/mK. We set the pre-intrusion geothermal gradient at 30 °C/km and introduced the magma as a single horizontal sheet, 3 km thick, with its top at 10 km depth. The magma, with $\rho = 2200$ kg/m^3, Cp = 1100 J/kgK and $k = 3$ W/mK, was set to be internally convecting but cooling purely by conduction into zero-porosity wall rocks. For magma at an initial temperature of 1100 °C, the maximum temperatures at the upper and lower contacts were computed as 754 and 803 °C, respectively. The H_2O-saturated solidus in the Ab-Qtz-H_2O system (a model for tonalites and trondhjemites such as the wall rocks in this case) lies at 734 °C at 260 MPa, the calculated pressure of intrusion. For this model, the solidus would lie at 45 and 178 m from the upper and lower contacts, respectively. Because of the abundance of quartz and plagioclase in the wall rocks, a large amount of melt would be formed. In contrast, a model in which all parameters were the same, except that the initial magma temperature was set at 900 °C, produced peak upper and lower contact temperatures of only 658 and 708 °C, well below the solidus. In practice the 900 °C model would actually predict a very small degree of melting at the base of the intrusion. This is because the wall rocks contain a small amount of alkali feldspar and the first melting reaction would be at the H_2O-saturated solidus in Ab–Or–Qtz–H_2O. Allowing convection in the wall rocks, with a porosity of 0.1, increases the maximum temperatures by a few degrees. Thus, an intrusion initially at 900 °C would not produce enough melt to explain the presence of a significant metatexite zone, let alone a diatexite in the aureole. Intrusion temperatures would need to be much higher than 900 °C and more like 1100 °C in order to explain the observed migmatisation of the country rocks.

5. Discussion and conclusions

The present experiments suggest that the K-adakite magmas were generated at $P > 2$ GPa. The near-liquidus clinopyroxene in the K-adakite switches from being broadly augitic to omphacitic at $P > 1.5$ GPa, and the Jd component increases with P. Plagioclase disappears from the near-liquidus assemblage at some pressure between 2 and 2.5 GPa (Table 2). Also, the melts

produced in fluid-absent partial melting experiments on most starting materials become markedly more potassic within this pressure range. The 2.5 GPa melts coexist with Pl-free (eclogitic) assemblages of Grt+omphacite (Omp). Various aspects and the *P-T* location of the transition between garnet amphibolite/granulite and eclogite (in mafic rock systems) have been studied in several experimental studies (e.g., Green and Ringwood, 1967; Ito and Kennedy, 1971; Lambert and Wyllie, 1972; Rapp et al., 1991; Nair and Chacko, 2004). The transition is defined as the point of disappearance of plagioclase in the mineral assemblage. Plagioclase coexists with omphacitic pyroxene and garnet over a wide pressure interval (at 800 to 1100 °C). Its final disappearance requires pressures of at least 1.7 GPa, and many studies would place the minimum $P>2$ GPa, depending on the rock composition and the fluid regime involved. In more felsic rock systems, the elimination of plagioclase seems to require pressures similar those for the mafic rock systems (e.g., Patiño Douce, 2005). All this experimental evidence suggests that one essential element in the production of K-adakite melt, as opposed to more sodic magmas, is the higher pressures at which the melting reactions took place. It appears that the protoliths do not have to be very highly potassic rocks such as the shoshonite that we studied. Indeed our results suggest that the melts derived from a shoshonitic source rock would be syenitic rather than broadly granitic. Likewise, most basaltic compositions (tholeiites, olivine tholeiites, high-Al tholeiites and olivine basalts) are unsuitable source rocks because they produce melts that generally remain both too sodic ($K_2O/Na_2O \leq 0.84$) and commonly also highly peraluminous (see e.g., Rapp et al., 1991; Rapp and Watson, 1995; Skjerlie and Patiño Douce, 2002). More potassic metabasalts/gabbros, metadiorites and metatonalites, however, could be suitable source rocks for both ordinary adakites as well as the K-rich varieties, with the pressure of partial melting governing whether the melts would be ordinary or K-rich adakites. For example, Antignano and Rushmer (2002) produced melts with adakitic chemistry by fluid-absent partial melting of a potassic metadiorite, at 950 °C and 1.4 GPa. The alkali basaltic starting material used by Sen and Dunn (1994) produced melts with K_2O/Na_2O comparable to those of K-adakites at $P=1.5$ and 2 GPa, but only at relatively low T (≤ 950 °C). The implications of the very high pressures involved in K-adakite genesis are discussed later.

The high temperatures inferred for generation of the K-rich adakite magmas (>1050 and probably ~1080 °C) may seem surprising. However, non-peralkaline, felsic volcanic rocks with emplacement temperatures up to 1100 °C are widely distributed in both space and geological time (see e.g., Table 2 of Henry and Wolff, 1992). In this respect, the K-adakites are simply intrusive examples of such high-*T* silicic magmas. The inferred *P* and *T* conditions for the genesis of the K-adakites imply an average geothermal gradient of around 13.5 °C/km (44 °C/kb). Such a gradient strongly implies the involvement of high mantle heat flow during magma genesis during orogenic collapse.

The relatively high, inferred, initial H_2O contents of the C-type adakite magmas constitute an argument against the model of their formation through crustal assimilation by mafic magma (c.f., the lower H_2O contents inferred for felsic magmas formed by assimilation; McCarthy and Patiño Douce, 1997). Instead, these high melt H_2O contents are best explained with magma formation by fluid-absent partial melting, involving the breakdown of zoisite (e.g., Skjerlie and Patiño Douce, 2002; Patiño Douce, 2005), at unusually high pressures (>2 GPa). At a pressure of 2.5 GPa and 1080 °C, a granitic melt would contain 6 wt% H_2O for $a H_2O = 0.3$ (Burnham, 1981). This is within the normal range of $a H_2O$ found for fluid-absent melting at lower pressures in the crust (e.g., Johannes and Holtz, 1996). Such a melt would only become H_2O-saturated at about 240 MPa, i.e., in the shallow crust, at roughly 9 km depth (c.f. the inferred emplacement depth of ~10 km). Thus, such a melt would have a high degree of mobility, as long as it was efficiently segregated from its restitic complements (Clemens and Droop, 1998).

In summary, the Chinese C-type, high-K, adakitic magmas were most probably generated from ancient igneous crustal sources (possibly TTG rocks) by high-*T* partial melting during the post-orogenic phase following extreme crustal thickening. The Tiantangzhai monzogranite has low MgO (1.00 wt%) and Mg# (34), and low Ni and Cr contents (Table 1), and is similar in chemistry to the high-SiO_2 adakites (Martin et al., 2005). We infer that the K-adakite magma cannot have interacted significantly with mantle rocks during its ascent through the lithosphere (see e.g., Rapp et al., 1999; Martin et al., 2005). This means that, if the source rocks were eclogite-facies materials that delaminated from the over-thickened crust and foundered into the lithosphere, the adakite protolith remained near the base of the crust, with little mantle material above it. It is perhaps more likely that the K-adakitic melts were simply derived from the base of the over-thickened crust. Delamination may well have occurred, but the K-adakite protolith either remained attached to the crustal root or did not sink far into the mantle. The melting reactions most probably

involved the breakdown of zoisite, to produce quite hydrous but strongly H_2O-undersaturated melts coexisting with a residuum dominated by garnet and omphacitic pyroxene, but with minor rutile and apatite. Magma emplacement was most probably in the middle crust, at about 10 km depth.

Acknowledgements

This study was financially supported by the National Science Foundation of China (grants 40472037 and 40334037) and the Royal Society, UK (through grants for an International Incoming Short Visit to the UK for XL and an International Outgoing Short Visit to China, for JDC). The authors thank Mr W. Edwards and Mr R. Giddens for assistance in obtaining SEM images and electron probe analyses of the experimental run products, as well as some analyses of the minerals in the starting rocks used in the experimental study. Mr Xu Haijing provided some analytical data on the K-adakite starting material as well as guidance in the field. Dr Wang Qiang provided us with the shoshonite sample used in some of the experiments.

References

Abbott Jr., R.N., 1981. AFM liquidus projections for granitic magmas, with special reference to hornblende, biotite and garnet. Can. Mineral. 19, 103–110.

Anderson, J.L., Smith, D.R., 1995. The effects of temperature and fO_2 on the Al-in-hornblende barometer. Am. Mineral. 80, 549–559.

Atherton, M.P., Petford, N., 1993. Generation of sodium-rich magmas from newly underplated basaltic crust. Nature 362, 144–146.

Antignano, A.V., Rushmer, T., 2002. Tonalite generation in arc regimes: results from metadiorite partial melting experiments. Goldschmidt Conference Abstracts, p. A24.

Beate, B., et al., 2001. Mio-Pliocene adakite generation related to flat subduction in southern Ecuador: the Quimsacocha volcanic center. Earth Planet. Sci. Lett. 192, 561–570.

Bédard, J.H., 2006. A catalytic delamination-driven model for coupled genesis of Archaean crust and sub-continental lithospheric mantle. Geochim. Cosmochim. Acta 70, 1188–1214.

Bindeman, I.N., Eiler, J.M., Yogodzinski, G.M., Tatsumi, Y., Sterne, C.R., Grove, T.L., Portnyagin, M., Hoernle, K., Danyushevsky, L.V., 2005. Oxygen isotope evidence for slab melting in modern and ancient subduction zones. Earth Planet. Sci. Lett. 235, 480–496.

Bourdon, E., et al., 2002. Adakite-like lavas from Antisana volcano (Ecuador): Evidence for slab melt metasomatism beneath the Andean Northern Volcanic Zone. J. Petrol. 43, 199–217.

Burnham, C.W., 1981. The nature of multicomponent aluminosilicate melts. Phys. Chem. Earth 13, 197–229.

Calmus, T., et al., 2003. Spatial and temporal evolution of basalts and magnesian andesites ("bajaites") from Baja California, Mexico: the role of slab melts. Lithos 66, 77–105.

Castillo, P.R., 2006. An overview of adakite petrogenesis. Chin. Sci. Bull. 51, 257–268.

Cawthorn, R.G., O'Hara, M.J., 1976. Amphibole fractionation in calc-alkaline magma genesis. Am. J. Sci. 276, 309–329.

Chen, N.S., You, Z.D., Suo, S.T., Yang, Y., Li, H.M., 1996. The U–Pb age of the Dabie intermediate to felsic granulites and deformed granites. Chin. Sci. Bull. 41, 1009–1012.

Chen, B., Jahn, B-M., Wei, C.J., 2002. Petrogenesis of Mesozoic granitoids in the Dabie UHP complex, central China: trace element and Nd-Sr isotopic evidence. Lithos 60, 67–88.

Clemens, J.D., 2003. S-type granitic magmas — petrogenetic issues, models and evidence. Earth-Sci. Rev. 61, 1–18.

Clemens, J.D., Droop, G.T.R., 1998. Fluids, *P-T* paths and the fates of anatectic melts in the Earth's crust. Lithos 44, 21–36.

Clemens, J.D., Holness, M.B., 2000. Textural evolution and partial melting of arkose in a contact aureole: a case study and implications. Electron. Geosci. (now Vis. Geosci.) 5 (4).

Clemens, J.D., Mawer, C.K., 1992. Granitic magma transport by fracture propagation. Tectonophysics 204, 339–360.

Clemens, J.D., Petford, N., 1999. Granitic melt viscosity and silicic magma dynamics in contrasting tectonic settings. J. Geol. Soc. Lond. 156, 1057–1060.

Clemens, J.D., Watkins, J.M., 2001. The fluid regime of high-temperature metamorphism during granitoid magma genesis. Contrib. Mineral. Petrol. 140, 600–606.

Devine, J.D., Gardner, J.E., Brack, H.P., Layne, G.D., Rutherford, M.J., 1995. Comparison of microanalytical methods for estimating H_2O contents of silicic volcanic glasses. Am. Mineral. 80, 319–328.

Defant, M.J., Drummond, M.S., 1990. Derivation of some modern arc magmas by melting of young subducted lithosphere. Nature 347, 662–665.

Drummond, M.S., Defant, M.J., 1990. A model for trondhjemite–tonalite–dacite genesis and crustal growth via slab melting: Archean to modern comparisons. J. Geophys. Res. [Solid Earth] 95, 21503–21521.

Finger, F., Clemens, J.D., 1995. Migmatization and "secondary" granitic magmas: effects of emplacement of "primary" granitoids in Southern Bohemia, Austria. Contrib. Mineral. Petrol. 120, 311–326.

Foley, S., Tiepolo, M., Vannucci, R., 2002. Growth of early continental crust controlled by melting of amphibolite in subduction zones. Nature 417, 837–840.

Graphchikov, A.A., Konilov, A.N., Clemens, J.D., 1999. Biotite dehydration, partial melting, and fluid composition: experiments in the system $KAlO_2$–FeO–MgO–SiO_2–H_2O–CO_2. Am. Mineral. 84, 15–26.

Green, D.H., Ringwood, A.E., 1967. An experimental investigation of the gabbro to eclogite transformation and its petrological applications. Geochim. Cosmochim. Acta 31, 767–783.

Gutscher, M.A., Maury, R., Eissen, J.P., Bourdon, E., 2000. Can slab melting be caused by flat subduction? Geology 28, 535–538.

Henry, C.D., Wolff, J.A., 1992. Distinguishing strongly rheomorphic tuffs from extensive silicic lavas. Bull. Volcanol. 54, 171–186.

Holness, M.B., Clemens, J.D., 1999. Partial melting of the Appin 'Quartzite' driven by fracture-controlled H_2O infiltration in the aureole of the Ballachulish Igneous Complex, Scottish Highlands. Contrib. Mineral. Petrol. 136, 154–168.

Ito, K., Kennedy, G.C., 1971. An experimental study of the basalt–garnet granulite–eclogite transition. In: Heacock, G. (Ed.), The Structure and Physical Properties of the Earth's Crust. Geophys. Monogr. Am. Geophys. U., vol. 14, pp. 303–314.

Johannes, W., Holtz, F., 1996. Petrogenesis and Experimental Petrology of Granitic Rocks. Springer-Verlag, Berlin. 335 pp.

Kretz, R., 1983. Symbols for rock-forming minerals. Am. Mineral. 68, 277–279.

Kushiro, I., Yoder Jr., H.S., 1972. Origin of the calc-alkaline peraluminous andesites and dacites. Carnegie Inst. Wash. Yearb., vol. 71, pp. 411–413.

Lambert, I.B., Wyllie, P.J., 1972. Melting of gabbro (quartz eclogite) with excess water to 35 kilobars, with geological applications. J. Geol. 80, 693–708.

LeBreton, N., Thompson, A.B., 1988. Fluid-absent (dehydration) melting of biotite in metapelites in the early stages of crustal anatexis. Contrib. Mineral. Petrol. 99, 226–237.

Ma, C.Q., Li, Z.C., Ehlers, C.A., 1998. Post-collisional magmatic plumbing system: Mesozoic granitoid plutons from the Dabieshan high-pressure and ultrahigh-pressure metamorphic zone, eastern-central China. Lithos 45, 431–456.

Macpherson, C.G., Dreher, S.T., Thirlwall, M.F., 2006. Adakites without slab melting: high pressure differentiation of island arc magma, Mindanao, the Philippines. Earth Planet. Sci. Lett. 243, 581–593.

Martin, H., Smithies, R.H., Rapp, R., Moyen, J.F., Champion, D., 2005. An overview of adakite, tonalite–trondhjemite–granodiorite (TTG), and sanukitoid: relationships and some implications for crustal evolution. Lithos 79 (1–2), 1–24.

McCaffrey, K.J.W., Petford, N., 1997. Are granitic intrusions scale invariant? J. Geol. Soc. Lond. 154, 1–4.

McCarthy, T.C., Patiño Douce, A.E., 1997. Experimental evidence for high-temperature felsic melts formed during basaltic intrusion of the deep crust. Geology 25, 463–466.

Moyen, J.-F., Stevens, G., 2005. Experimental constraints on TTG petrogenesis: implications for Archean geodynamics. In: Benn, K., Mareschal, J-C., Condie, K.C. (Eds.), Archean Geodynamics and Environments. AGU Monograph Series, vol. 164, pp. 149–175.

Nair, R.K., Chacko, T., 2004. Experimental constraints on amphibolite/granulite–eclogite transition in metabasalts: implications for slab melting in warm subduction zones. GSA Annual Meeting. Paper, vol. 195–8. Geol. Soc. Am., Denver.

Patiño Douce, A.E., 2005. Vapor-absent melting of tonalite at 15–32 kbar. J. Petrol. 46, 275–290.

Patiño Douce, A.E., Beard, J.S., 1995. Dehydration-melting of biotite gneiss and quartz amphibolite from 3 to 15 kbar. J. Petrol. 36, 707–738.

Peacock, S.M., Rushmer, T., Thompson, A.B., 1994. Partial melting of subducting oceanic-crust. Earth Planet. Sci. Lett. 121, 227–244.

Petford, N., Cruden, A.R., McCaffrey, K.J.W., Vigneresse, J-L., 2000. Granite magma formation, transport and emplacement in the Earth's crust. Nature 408, 669–673.

Powers, R.E., Bohlen, S.R., 1985. The role of synmetamorphic igneous rocks in the metamorphism and partial melting of metasediments, Northwest Adirondacks. Contrib. Mineral. Petrol. 90, 401–409.

Rapp, R.P., 1995. Amphibole-out phase-boundary in partially melted metabasalt, its control over liquid fraction and composition, and source permeability. J. Geophys. Res. [Solid Earth] B100, 15601–15610.

Rapp, R.P., Watson, E.B., 1995. Dehydration melting of metabasalt at 8–32 kbar: implications for continental growth and crust–mantle recycling. J. Petrol. 36, 891–931.

Rapp, R.P., Watson, E.B., Miller, C.F., 1991. Partial melting of amphibolite/eclogite and the origin of Archean trondhjemites and tholeiites. Precambrian Res. 51, 1–25.

Rapp, R.P., Shimizu, N., Norman, M.D., Applegate, G.S., 1999. Reaction between slab-derived melts and peridotite in the mantle wedge: experimental constraints at 3.8 GPa. Chem. Geol. 160, 335–356.

Rapp, R.P., Xiao, L., Shimizu, N., 2002. Experimental constraints on the origin of potassium-rich adakites in eastern China. Acta Pet. Sin. 18, 293–302.

Rollinson, H.R., 1993. Using Geochemical Data: Evaluation, Presentation, Interpretation. Longman Scientific & Technical, London. 352 pp.

Sajona, F.G., et al., 1993. Initiation of subduction and the generation of slab melts in Western and Eastern Mindanao, Philippines. Geology 21, 1007–1010.

Sajona, F.G., et al., 1994. Magmatic response to abrupt changes in geodynamic settings — Pliocene Quaternary Calc-Alkaline and Nb-Enriched Lavas from Mindanao (Philippines). Tectonophysics 237, 47–72.

Sajona, F.G., et al., 2000. Magmatic source enrichment by slab-derived melts in a young post-collision setting, central Mindanao (Philippines). Lithos 54, 173–206.

Scaillet, B., Holtz, F., Pichavant, M., 1998. Phase equilibrium constraints on the viscosity of silicic magmas — 1. Volcanic-plutonic association. J. Geophys. Res. [Solid Earth] 103, 27257–27266.

Sen, C., Dunn, T., 1994. Dehydration melting of a basaltic composition amphibolite at 1.5 and 2.0 GPa: implications for the origin of adakites. Contrib. Mineral. Petrol. 117, 394–409.

Sisson, T.W., Ratajeski, K., Hankins, W.B., Glazner, A.F., 2005. Voluminous granitic magmas from common basaltic sources. Contrib. Mineral. Petrol. 148, 635–661.

Skjerlie, K.P., Patiño Douce, A.E., 2002. The fluid-absent partial melting of a zoisite-bearing quartz eclogite from 1.0 to 3.2 GPa; implications for melting in thickened continental crust and for subduction-zone processes. J. Petrol. 43, 291–314.

Stevenson, J.A., Daczko, N.R., Clarke, G.L., Pearson, N., Klepeis, K.A., 2005. Direct observation of adakite melts generated in the lower continental crust, Fiordland, New Zealand. Terra Nova 17, 73–79.

Stimac, J., Hickmott, D., 1994. Trace-element partition-coefficients for ilmenite, ortho-pyroxene and pyrrhotite in rhyolite determined by micro-pixe analysis. Chem. Geol. 117, 313–330.

Taylor, S.R., McLennan, S.M., 1985. The Continental Crust: its Composition and Evolution. Blackwell Scientific Publications, Oxford. 312 pp.

Thompson, A.B., Ellis, D.J., 1994. $CaO+MgO+Al_2O_3+SiO_2+H_2O$ to 35 kb — amphibole, talc, and zoisite dehydration and melting reactions in the silica-excess part of the system and their possible significance in subduction zones, amphibolite melting, and magma fractionation. Am. J. Sci. 294, 1229–1289.

Truckenbrodt, J., Ziegenbein, D., Johannes, W., 1997. Redox conditions in piston-cylinder apparatus: the different behavior of boron nitride and unfired pyrophyllite assemblies. Am. Mineral. 82, 337–344.

Wang, R.J., Wang, Q., He, Y., 1998. Petrogenesis and age of the Jiuzihe-Tiantangzhai granite at the core of the Dabieshan orogenic belt. Bull. Mineral. Petrol. Chem. 17, 224–228 (in Chinese with English abstract).

Wang, Q., Qiu, J., Wang, R., 2000. The formation of Yangshanian granitic magma in the Dabie Mountains: dehydration or aquifer melting — with the Tiantangzhai and Jiuzihe granites as examples. Acta Geol. Sin. 74, 63–71 (in Chinese with English abstract).

Wang, Q., Wyman, D.A., Xu, J.F., Zhao, Z.H., Ping, J., Xiong, X.L., Bao, Z.W., Li, C.F., Bai, Z.H., 2006. Petrogenesis of Cretaceous adakitic and shoshonitic igneous rocks in the Luzong area, Anhui Province (eastern China): Implications for geodynamics and Cu–Au mineralization. Lithos 89, 424–446.

We, C.J., Zhang, L.F., Wang, G., 2001. Mesozoic high-K granitic rocks from the eastern Dabie Mountains, central China and their geological implications. Sci. China, Ser. D 44, 525–534.

Winther, K.T., 1996. An experimentally based model for the origin of tonalitic and trondhjemitic melts. Chem. Geol. 127, 43–59.

Winther, K.T., Newton, R.C., 1991. Experimental melting of hydrous low-K tholeiite: evidence on the origin of Archaean cratons. Bull. Geol. Soc. Den. 39, 213–228.

Wohlerz, K., Heiken, G., 1991. Volcanology and Geothermal Energy. University of California Press. 432 pp.

Xiao, L., Rapp, R.P., Xu, J.F., 2004. The role of deep processes controls on variation of compositions of adakitic rocks. Acta Petrol. Sin. 20, 219–228.

Xiao, L., Zhang, H.F., Clemens, J.D., Wang, Q.W., 2006. Late Triassic granitoids of the eastern margin of the Tibetan Plateau: petrogenesis and implications for tectonic evolution. Lithos in review.

Xiong, X.L., in press. Trace element evidence for growth of early continental crust by melting of rutile-bearing hydrous eclogite. Geology.

Xiong, X.L., Adam, T.J., Green, T.H., 2005. Rutile stability and rutile/melt HFSE partitioning during partial melting of hydrous basalt: implications for TTG genesis. Chem. Geol. 218, 339–359.

Xu, H.J., 2005. Late Mesozoic magmatic intrusion sequences of the central Dabie Orogenic belt, China: implication for the transition of tectonic regimes. PhD thesis (unpublished), China University of Geosciences, Wuhan, 130 pp.

Xu, J.F., Shinjo, R., Defant, M.J., Wang, Q.A., Rapp, R.P., 2002. Origin of Mesozoic adakitic intrusive rocks in the Ningzhen area of east China: partial melting of delaminated lower continental crust? Geology 30, 1111–1114.

Yan, Q.S., 2005. Rock associations and its evolution of Bixiling and Sidaohe area in UHP metamorphic terrene, Dabie Mountains. MSc dissertation (unpublished), China University of Geosciences, Wuhan, 62 pp.

Yogodzinski, G.M., et al., 2001. Geochemical evidence for the melting of subducting oceanic lithosphere at plate edges. Nature 409, 500–504.

Zhang, Q., Wang, Y., Wang, Y.L., 2001. Preliminary study on the components of the lower crust in east China Plateau during Yangshanian Period: constraints on Sr and Nd isotopic compositions of adakite-like rocks. Acta Petrol. Sin. 17, 505–513.

Zhang, H.F., Zhang, L., Harris, N., Jin, L.L., Yuan, H.L., Zhang, B.R., 2006. U–Pb zircon ages, geochemical and isotopic compositions of granitoids in Songpan-Garzê Fold Belt, eastern Tibet Plateau: Constraints on petrogenesis, nature of basement and tectonic evolution. Contrib. Mineral. Petrol. 152, 75–88.

Zhang, H.F., Xiao, L., Zhang, L., Yuan, H.L., Jin, L.L., in press. Geochemical and Pb–Sr–Nd isotopic compositions of Indosinian granitoids from the Bikou block, northwest of the Yangtze plate: constraints on petrogenesis, nature of deep crust and geodynamics. Science in China.